

# Electrical Resistivity Survey to Delineate Groundwater Potential Zones in Granitic Terrain, Nalgonda District, India

**Ratnakar Dhakate\*, B.C. Negi and V.S. Singh**

National Geophysical Research Institute

Hyderabad – 500 007, India

✉ dhakate\_ratnakar@yahoo.com

*Received November 3, 2005; revised and accepted December 26, 2006*

**Abstract:** Vertical Electrical Soundings (VES) with Schlumberger configuration were conducted in order to delineate groundwater potential aquifer zones in Wailpally watershed area, Nalgonda district, Andhra Pradesh, India. The entire area is underlain by granite and gneissic complex. Locating favourable groundwater zones in granitic terrain is a very difficult task, as the secondary features developed in hard rocks like faults, fractures, lineaments and dykes control the groundwater flow and movement. Therefore, there is always a need for locating and pinpointing the favourable location in hard rock areas. In order to assess groundwater potential zones, 59 vertical electrical soundings (VES) with 100 to 200 m current electrode separation were conducted in the watershed area. Interpreted VES data were correlated with the drilled borehole logs and used to generate iso-resistivity maps like top layer resistivity, depth to the bed rock and longitudinal unit conductance maps. Based on VES interpreted data groundwater potential maps have been prepared showing good, moderate and poor zones.

**Key words:** Vertical electrical sounding (VES), groundwater potential, pinpointing.

## Introduction

Groundwater exploration is becoming more and more important now-a-days to meet the increasing demand of water supply, especially in areas with inadequate surfacewater supply and in rural areas. The watershed area under study is about 80 km away from Hyderabad, the capital city of Andhra Pradesh and falls under chronic drought-prone area under Nalgonda district. The whole Wailpally watershed is underlain by hard rock like granite and gneisses complex. Due to differential weathering and fracturing, the aquifers in the hard rock terrain show wide variation both vertically and horizontally in their hydraulic characteristics and very useful for its aerial distribution for future development of groundwater potential zones (Yadav and Lal, 1989). Many wells in

the area drilled without proper investigation are failed or abandoned. Therefore, a systematic and scientific approach is essential to overcome these problems. The hard rock areas are known for low yield due to the absence of primary porosity; the groundwater in such areas are controlled by the secondary features like lineament, fractures, faults and dyke. Therefore, there is a need to locate such features for groundwater prospective.

In order to assess location of the favourable zones in northern part of the watershed, 59 vertical electrical soundings (VES) have been carried out with maximum of half current electrode separation ( $AB/2$ ) 100 to 200 m, which is widely used for groundwater exploration studies (Todd, 1959). This method is least expensive among all the geophysical methods and easy to operate. This method will give much more resistivity contrast from top layer to that of water-bearing formation and basement rock (Zohdy, 1974). This method is well suited

\*Corresponding Author

for groundwater studies in hard rock terrains (Bhimasankaram, 1970; Bhimasankaram and Gaur, 1977). Based on vertical electrical soundings and measuring nearby water level a groundwater potential map has been prepared.

### Brief Geology of the Study Area

The Wailpally watershed area lies in the Nalgonda district in Andhra Pradesh. In western region the area is covered by hilly slopes. The soil types are red sandy, sandy and loamy soils, and few patches of black cotton soils are also found in different places. Achaeans group of rocks, mainly consisting of granites and gneisses, underlies the investigated area. The granites are mostly pink and grey. The textures of rocks observed were medium to coarse grained. The pink granites are predominantly spread over the entire area with quartz and feldspars as essential minerals. The dykes are observed in few places and are exposed in some places. The geological map of the study area is shown in Figure 1.

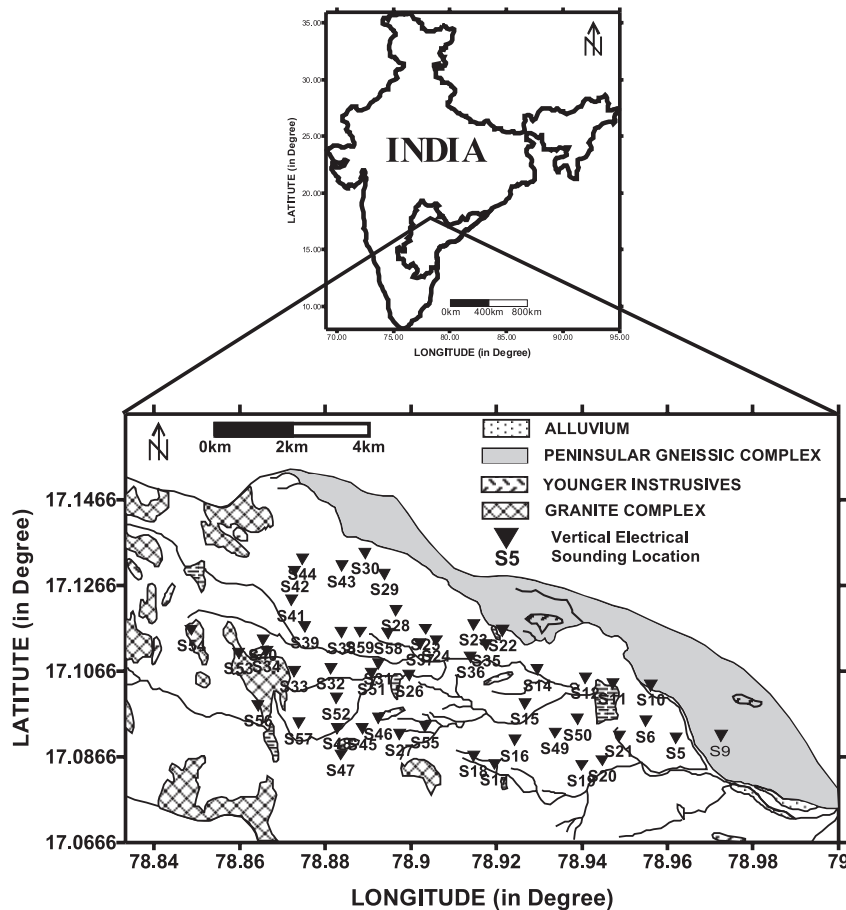


**Figure 1: Key map of the study area showing geology and vertical electrical sounding locations.**

### Geophysical Survey

Geophysical exploration mainly comprises measurements and interpretation of signals from natural or induced physical phenomena generated as a result of spatial changes in one or more physical properties of a sub-surface formation. These signals—measured repetitively at several points in space and time—are appropriately interpreted, considering the available geological information, in terms of subsurface structures/features which may themselves have good groundwater potential or indicative of good aquifers. Electrical resistivity method is the most widely applied method for groundwater prospecting. This is because of its efficacy to detect the water-bearing layers, besides being simple and inexpensive to carry out the field investigations (Zohdy, 1974). In general, for measuring resistivities of subsurface formations, four electrodes are required. A current of electrical intensity ( $I$ ) is introduced between one pair of electrodes, called current electrodes. The current electrodes can be identified as A and B and sometimes  $+I$  and  $-I$  denoting source and sink

respectively. The potential difference produced as a result of current flow is measured with the help of another pair of electrodes, called potential electrodes or probes. The potential electrodes may be represented as M and N.

### Schlumberger Array

This array also uses four collinear point electrodes, but measures the potential gradient at the mid-point by keeping the measuring electrodes close to each other. Four electrodes are placed along a straight line symmetrically over centre point 'O'. Current ( $I$ ) is sent through the outer current electrodes A and B and the potential is measured across inner potential electrodes M and N. The separation between the potential electrodes is kept small as compared to the current electrodes separation ( $MN < 1/5 AB$ ).

The configuration or geometric factor for the Schlumberger array is given by

$$G = \frac{(AB/2)^2 - (MN/2)^2}{(MN/2)} \frac{\pi}{2}$$

where AB is the distance between current electrodes, MN is the distance between

potential electrodes, and the apparent resistivity is obtained with the formula

$$\rho_a = G (\Delta V/I)$$

where  $(\Delta V/I)$  is the potential difference between potential electrodes to that of current flowing.

Depending upon whether the apparent resistivity value increases or decreases with each electrode separation, the shape of the curve is changed and this curve is helpful for quantitative interpretation of the electrical resistivity data. The qualitative interpretation of the subsurface layer resistivity distribution can be observed from the shape of the curve. A curve is drawn by plotting the observed apparent resistivity values against the current electrode separation on a log-log graph sheet, and this is interpreted by matching the field curve with master curves of two-, three- and four-layer cases for various ratios of absolute resistivity given off (Orellana and Mooney, 1966). The three-layered earth model can be classified into A, Q, H and K type curves based on the shape. The resistivity distribution for three-layered curve is as follows:

A-type:  $\rho_1 < \rho_2 < \rho_3$ ;

Q-type:  $\rho_1 > \rho_2 > \rho_3$ ;

H-type:  $\rho_1 > \rho_2 < \rho_3$ ;

K-type:  $\rho_1 < \rho_2 > \rho_3$ .

Similarly, four-layer curves are AA, QQ, HK, KH, HA, KQ, AK and QH.

## Result and Discussion

Fifty-nine vertical electrical soundings were conducted in the watershed and their locations are shown in Figure 1. The VES data are first interpreted using the curve matching technique (Orellana and Mooney, 1966) and then by Inversion Iteration Method (Jupp, 1975) the interpreted results of VES are given in Table 1. Three sounding curves show A-type three-layer geo-electrical section, while thirty three sounding curves show AA-type curve, fourteen sounding curves show HA-

type, nine curves show KH-type curve and only one curve shows QH-type suggesting four-layer geoelectrical section. The details of analysis of sounding curves is given in Table 2 and shown in Figure 2. The major type of curves obtained is predominantly AA type followed by HA and KH types as given in Table 2. Based on the interpreted results of vertical electrical sounding curves, the resistivity ranges of different subsurface layers are shown in Figure 2.

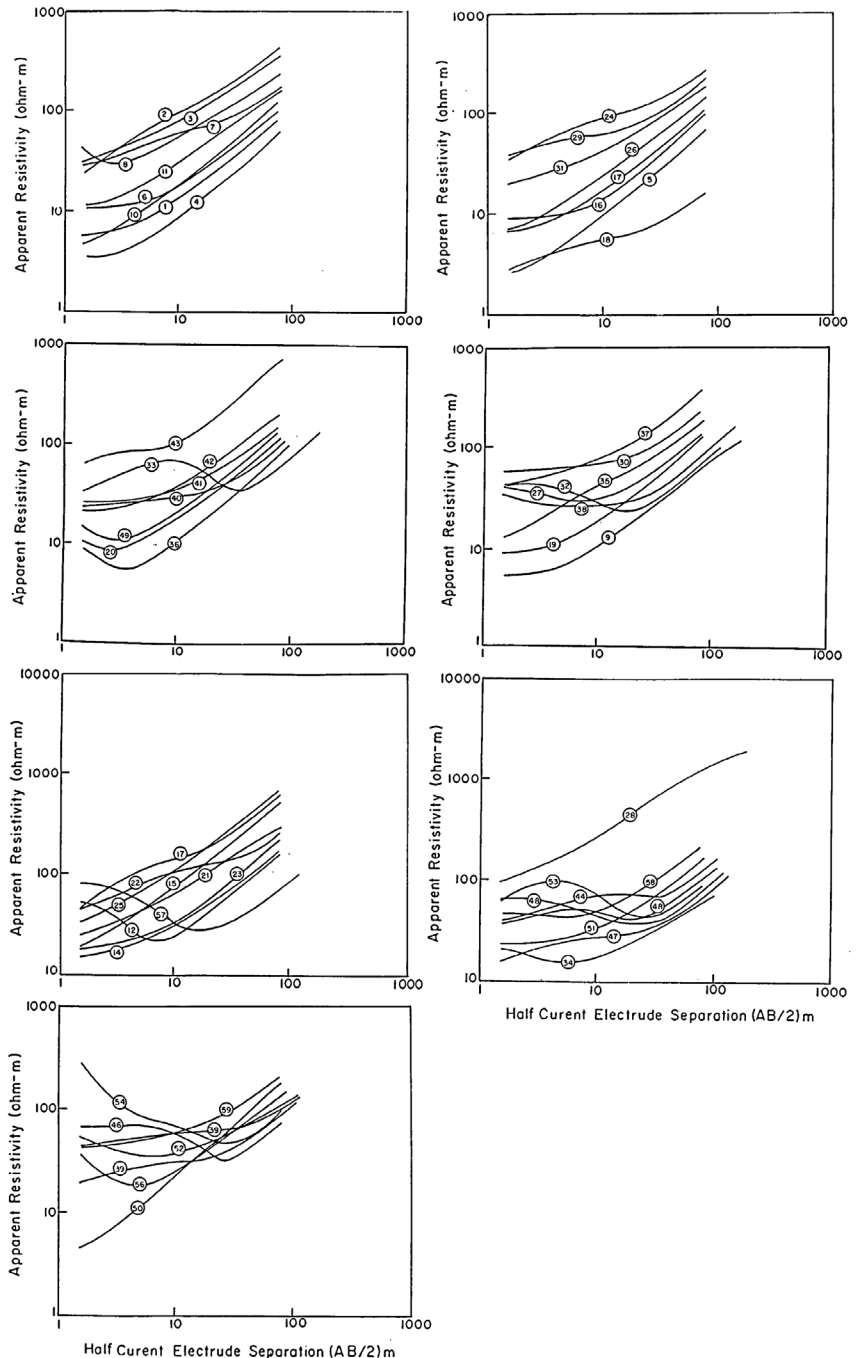


Figure 2: Vertical electrical sounding field curves.

**Table 1: Details of vertical electrical sounding and their interpreted results and apparent resistivity at different depths along with longitudinal unit conductance**

VES No.	Type of curve	Interpreted layer parameters										Total H $h_1+h_2+h_3+h_4$ (m)	Apparent resistivity at various depth (AB/2)				Longitudinal unit conductance (mhos)
		$\rho_1$	$h_1$	$\rho_2$	$h_2$	$\rho_3$	$h_3$	$\rho_4$	$h_4$	$\rho_5$	1.5		10	50	100		
		$\Omega\text{-m}$	m	$\Omega\text{-m}$	m	$\Omega\text{-m}$	m	$\Omega\text{-m}$	m	$\Omega\text{-m}$	(m)		(m)	(m)	(m)		
S1	AA	6	2.4	13	3.3	52	10	1178			15.7	5	12	52	120	0.87	
S2	KH	13	0.7	152	3.8	109	7.8	1944			12.3	22	92	303	518	0.15	
S3	AA	24	1.1	56.8	2.5	130.1	11	2007			13.36	30	80	254	452	0.15	
S4	A	3.3	2.4	7.8	3.1	60.6	8.2	1211			13.6	4	9	38	82	1.25	
S5	AA	2.2	1.7	14.9	3.3	86.7	12.3	1203			17.3	3	10	42	89	1.13	
S6	A	10.3	5.9	156.1	33.9	9766					34.8	18	16	69	121	0.77	
S7	KH	27.3	1.8	82.7	7.4	46.5	9.4	752.5			18.6	27	58	123	216	0.35	
S8	HA	81.1	0.6	18.8	1.7	86.1	12.8	655			15.1	43	55	171	259	0.24	
S9	AA	5.2	4.3	35.3	4.4	110.1	18.4	190	8.6	481	25.2	6	10	47	68	1.08	
S10	AA	4.1	1.5	25.2	2	55.2	7.2	1849			10.7	5	19	83	159	0.57	
S11	AA	10.9	2.7	85.8	5.7	150.2	12	688.9			20.4	13	32	112	192	0.39	
S12	HA	54.9	1.8	8.9	3.1	171.1	6.9	333.4	12.6	1088	17.4	47	24	106	150	0.44	
S13	KH	23	0.6	237	3.4	99.9	8.1	7854			12.1	41	142	399	655	0.12	
S14	AA	14.2	1.6	28.1	4.8	84.8	13.2	1316			19.6	15	32	100	223	0.43	
S15	AA	12.9	0.8	49.8	2.4	207.2	5	3372			8.2	19	73	349	625	0.13	
S16	AA	9.1	6	37.8	2.6	186.9	5.1	3243			13.7	9	12	73	125	0.75	
S17	AA	6.3	2.1	17.7	3.8	85	11	1105			16.9	7	19	68	136	0.67	
S18	AA	22.6	1.1	65.5	5.6	57.4	8.9	96.3	8.5	573	26.3	28	58	113	199	0.38	
S19	AA	8.7	3.8	61.6	8.1	211.7	8.6	9868			20.5	9	14	85	149	0.60	
S20	HA	13.4	0.8	5.5	2	63.3	15.1	9929			17.9	10	19	76	149	0.66	
S21	AA	21.2	1.4	51.3	4.4	258.4	8.3	604.3			14.1	23	62	196	339	0.18	
S22	AA	41.9	1.6	141.6	14.9	105.6	13.6	255.7	8.8	9901	35	48	111	183	296	0.27	
S23	AA	16.5	1	24.4	5.4	124.3	6	315.6	7.3	11646	14	18	35	134	318	0.33	
S24	AA	28.8	1.1	112.2	17.6	216	10	1430			28.7	35	89	182	375	0.24	
S25	AA	27.1	1.1	93.4	2	185.9	5	372.4	7.9	12272	12.5	33	116	435	928	0.08	
S26	AA	6.3	1.9	57.3	4.5	121.2	18.1	9504			24.5	7	25	97	181	0.52	
S27	HA	45.1	1.3	27.4	8.9	95.8	16.5	197.7	10.2	9854	29.1	43	35	92	165	0.52	
S28	AA	64.4	0.7	186	3.7	438.3	3.5	2658			7.9	79	232	998	1489	0.03	
S29	AA	28.1	0.7	61.6	12.5	137.4	8.1	318.9	9.1	1870	26.5	36	62	149	307	0.30	
S30	AA	56.3	2.9	86.3	4.2	50.3	6	141.4	12.7	1685	28.8	62	72	148	308	0.31	
S31	AA	17.4	1	33.4	4.2	82.6	6	161	11.1	563	19.3	18	42	137	204	0.31	
S32	HA	44.5	4.3	15.5	12.9	120.9	11.1	212.2	13.9	1256	38.5	43	28	44	86	1.08	
S33	KH	24.6	0.9	102	5.7	15.9	18.2	1064			24.8	33	68	41	66	1.23	
S34	KA	22.7	1.2	12.9	5.3	42.7	25.3	65.5	5.9	331	38.6	21	16	39	76	1.22	

S35	AA	11.2	1.4	73.7	20.1	250.3	6	10118				27.5	13	46	119	246	0.42
S36	HA	14.6	0.7	3.7	2.7	23.3	3.4	200.3	5.7	13249		10	9	10	51	128	0.92
S36	AA	32.2	0.8	70.1	5.6	124.1	6.8	296.5	10	11337		19.5	39	77	241	551	0.16
S38	HA	112	0.4	27.5	21.7	87.6	5.8	297.9	9.6	4732		30.2	37	31	55	112	0.85
S39	AA	15.6	0.8	30	16.9	66.4	13.4	163.1	13.4	1297		34.1	19	30	55	103	0.81
S40	AA	23.1	1.7	32	17.6	127.3	13.5	1189				32.8	26	33	65	130	0.73
S41	A	25.2	4.8	61.7	16.2	726.5						21	27	37	99	175	0.45
S42	AA	20.2	2.4	38.2	5.5	129.7	9.1	892.4				17	20	37	136	234	0.33
S43	KH	38.5	0.6	130.8	1.6	41	2.9	387	4.3	17420		7.7	55	95	527	916	0.09
S44	KH	39.2	1.1	92.4	9.6	28.1	13.5	10477				24.2	39	70	82	150	0.61
S45	KH	34.2	1.4	72.1	3.7	23.5	14.2	715				19.3	37	48	70	120	0.69
S46	KH	63.4	1.9	79.7	4.6	15.5	14.4	1028	—	—		20.9	62	57	47	94	1.01
S47	AA	11.2	0.7	20.8	27.4	97.6	7	1000	—	—		35.1	15	28	47	84	1.45
S48	HA	64.2	3.9	31.1	24.3	68.9	12.3	9884	—	—		40.5	62	47	50	98	1.02
S49	HA	23.4	0.6	8.3	3.2	95.3	14	9990	—	—		17.8	15	20	92	180	0.55
S50	AA	3.8	1.5	37	1.7	183	4	11451	—	—		7.2	5	20	112	218	0.46
S51	AA	23	3.7	44.6	8.1	88.4	11.1	1205	—	—		22.9	27	34	98	188	0.46
S52	HA	62.3	0.9	30.4	6.8	71.3	32.1	560	—	—		39.8	51	34	70	123	0.68
S53	KH	34.4	0.6	179.1	2.3	32.5	22.5	284	—	—		25.4	60	67	57	106	0.72
S54	QH	316	1	69.7	8.6	24.3	18.3	9952	—	—		27.9	264	68	55	122	0.88
S55	AA	41.6	1.8	56.9	35.9	105.5	10.8	627	—	—		48.5	36	56	71	111	0.77
S56	HA	58.4	0.7	15.6	5.9	124.7	13.1	516	—	—		19.7	37	23	88	153	0.49
S57	HA	83.4	2.5	24.3	22.2	120.2	14.1	1283	—	—		38.9	73	31	45	86	1.06
S58	HA	47.8	1.9	35.7	3.7	77.1	12.1	1036.	—	—		17.7	43	50	141	275	0.30
S59	AA	37.5	0.9	49.4	5.5	76.7	14.2	951	—	—		20.6	40	52	135	242	0.32

**Table 2: Analysis of vertical electrical sounding**

Type of curve	Vertical electrical sounding numbers	Total numbers of curves
A-Type	4, 6, 41	3
AA-Type	1, 3, 5, 9, 10, 11, 14, 15, 16, 17, 18, 19, 21, 22, 23, 24, 25, 26, 28, 29, 30, 31, 35, 37, 39, 40, 42, 47, 50, 51, 55, 59,	32
KH-Type	2, 7, 13, 33, 43, 44, 45, 46, 53	9
HA-Type	8, 12, 20, 27, 32, 34, 36, 48, 49, 52, 56, 57, 58	14
QH-Type	54	1

2-65 Ohm-m	—	Top Soil Cover
20-100 Ohm-m	—	Weathered Formation
100-300 Ohm-m	—	Semi-weathered/dry fractures
>300 Ohm-m	—	Hard Rock

The apparent resistivity at different depths has been given in Table 1. Iso-resistivity contour maps at 1.5 m, 50 m and 100 m depths, as well as their 3-D maps were prepared, and they were interpreted in terms of resistivities and thicknesses of various subsurface layers.

### Top Layer Apparent Resistivity Map

The surface layer contour map along its 3-D view is given in Figure 3(a). The resistivity value ranges from 2-385  $\Omega$ -m, while its thickness ranges from 0.4-5.9 m. The variation in resistivity is mainly attributed to variation in moisture content and changes in surface conditions. The minimum resistivity of 2  $\Omega$ -m was observed in Yelmakana village at VES No. 5, while the maximum resistivity of 385  $\Omega$ -m is observed at Jangoan village at VES No. 43.

### Apparent Resistivity at 50 m Spacing

The apparent resistivity values for 50 m current electrode spacing ranging from 38-998  $\Omega$ -m, and the corresponding contour map with its 3-D view is given in Figure 3(b) with a contour interval of 50  $\Omega$ -m. The lowest apparent resistivity value of 38  $\Omega$ -m was observed in Yelmakana village at VES No. 4, while highest value of resistivity of 998  $\Omega$ -m was observed at Jangoan village at VES No. 28.

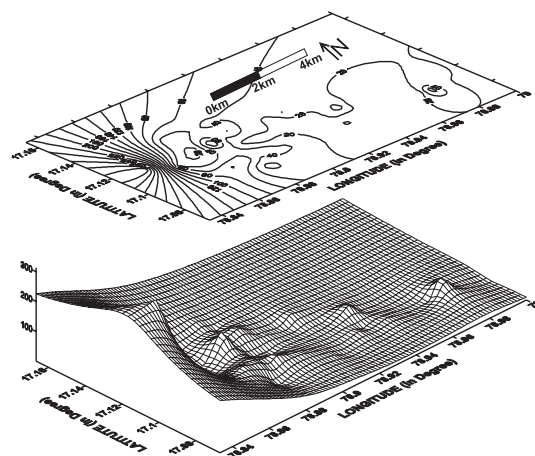
### Apparent Resistivity at 100 m Spacing

The apparent resistivity values for 100 m current electrode spacing ranging from 66-1489  $\Omega$ -m, and the corresponding contour map along its 3-D view is given in Figure 3(c) with a contour interval of 50  $\Omega$ -m. The lowest

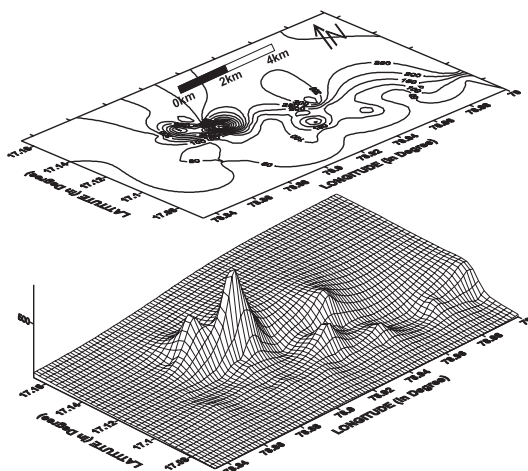
apparent resistivity value of 66  $\Omega$ -m was observed at Jangoan village at VES No. 33, while highest value of apparent resistivity of 1489  $\Omega$ -m was observed again at Jangoan village at VES No. 28.

### Longitudinal Conductance

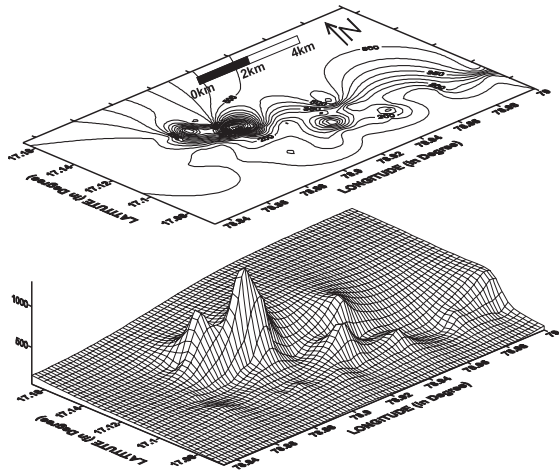
The ratio of different layers to their respective resistivities is known as the longitudinal conductance (Maillet, 1947). The properties of a thin conducting layer can be determined in terms of longitudinal conductance, and a resistive layer can be determined by transverse resistance which is the sum of product of resistivity and thickness (Maillet, 1947). Figure 4(d) depicts the total longitudinal conductance contour map along with its 3-D view. The conductance values in the area vary from 0.03 to 1.45. As the conductance value increases, the resistivity naturally decreases which point towards groundwater



(a) Apparent resistivity contour map with 3-D for top layer.



(b) Apparent resistivity contour map with 3-D at 50 m current electrode spacing.



**(d) Apparent resistivity contour map with 3-D for Longitudinal Unit Conductance.**

**Figure 3 (a, b, c and d): Apparent resistivity contour maps with 3-D representation.**

### Depth to the Basement

Information on depth to bedrock for an area is very necessary in order to estimate the thickness of the zone of saturation. The depth to the basement is useful for artificial/natural recharge to enhance the groundwater condition in the area. Chand et al. (2004) have estimated the natural recharge on its dependency using geoelectric

## Correlation of Results of Soundings with Lithology

The results of three resistivity sounding data (27, 32, 58) have been correlated with the drilled borewell logs as shown in Figure 4. Sounding no. 27 indicates four layers with resistivities 45, 27, 129 and 1029  $\Omega$ -m, with thickness 1.3, 9.8 and 18 m respectively. The first layer with resistivity 45  $\Omega$ -m indicates top soil; followed by second layer resistivity 27  $\Omega$ -m with thickness 9.8 m showing highly weathered rock upto a depth of 11.1 m; followed by a resistivity 129  $\Omega$ -m of semi-weathered nature upto a depth of 29.1 m; and the last layer resistivity shows very high value indicating hard rock, which is well correlating with the drilled borewell log. Similarly, sounding No. 32 shows four layers with resistivities 45, 15, 148 and 1246 with thickness 4.3, 12.7 and 21.5 m respectively. These layer parameters correlated with the drilled borewell log indicate that the first two layer resistivities i.e. 45 and 15  $\Omega$ -m represent weathered formation upto a depth of 17 m, followed by third layer resistivity 148 showing semi-weathered nature with thickness 21.5 m, and followed by hard rock with high resistivity. In case of sounding number 58, it also indicates four layer resistivities 48, 36, 77 and 1036  $\Omega$ -m with

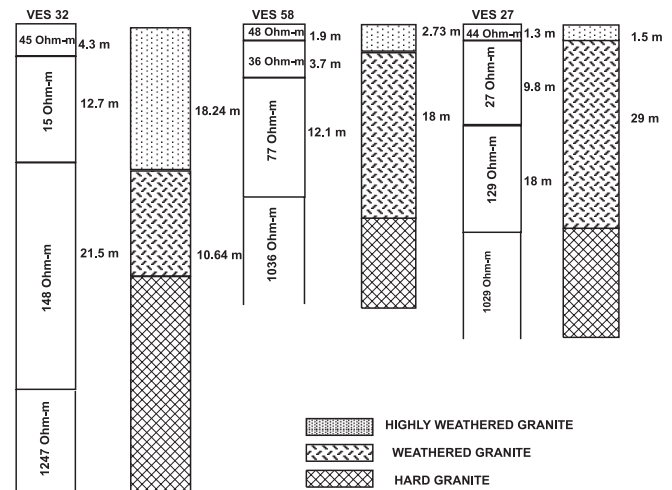


**Figure 4: Comparison of resistivity results with drilled borehole log data.**



thickness 1.9, 3.7 and 12.1 m respectively. When correlated with borewell log, it indicates that first layer resistivity 48  $\Omega$ -m top soil is followed by resistivities 36 and 77  $\Omega$ -m representing weathered formation with thickness 15.8 m followed by a hard rock.

### Groundwater Potential Aquifer Map

Considering the assumptions, the resistivity survey holds good both vertically and horizontally. The groundwater potential map has been prepared using the depth to bedrock map as shown in Figure 5. This map is classified into three areas i.e. poor, moderate and good zones. A shallow basement upto a depth of 20 m bgl with a minimum thickness of the saturated zone is classified as poor zone. A moderate groundwater zone is classified as the bedrock having a depth of 20-30 m bgl with average saturated thickness. This part is further used for artificial recharge to enhance the groundwater condition in the area. A good groundwater zone is classified as a bedrock having a depth of more than 30 m bgl and found in southern part of the watershed and at few places in isolated patches.

### Conclusions

Based on the resistivity surveys conducted in the area, the groundwater potential producing zones are identified. The study reveals that a large part of the area has poor to moderate groundwater producing potential. The

productive groundwater potential zone is only identified in the southern part and at few places in isolated patches. The drilled borehole logs are well correlated with resistivity data. Good prospects of groundwater development are in the study area where the depth to basement rock is relatively thick and has favourable low resistivity values and these areas can be further used for artificial recharge to enhance the groundwater conditions.

### Acknowledgement

Authors are grateful to Dr. V.P. Dimri, Director, N.G.R.I., Hyderabad for his continuous encouragement and kind permission to publish this paper.

### References

- Bhimasankaram, V.L.S., Bindi Madhav, U., Pantangay, N.S. and K.V. Ranga Rao (1970). Electrical resistivity investigation for groundwater in parts of Hyderabad district. Proc Sem Incidence of Aridity and Drought in Andhra Pradesh, Andhra University, Waltair.
- Bhimasankaram, V.L.S. and V.K. Gaur (1977). Lectures on exploration geophysics for geologists and engineers. Association of Exploration Geophysics, Centre for Exploration Geophysics, Hyderabad.
- Chand, R., Chandra, S., Rao, V.S., Singh, V.S. and S.C. Jain (2004). Estimation of natural recharge and its dependency

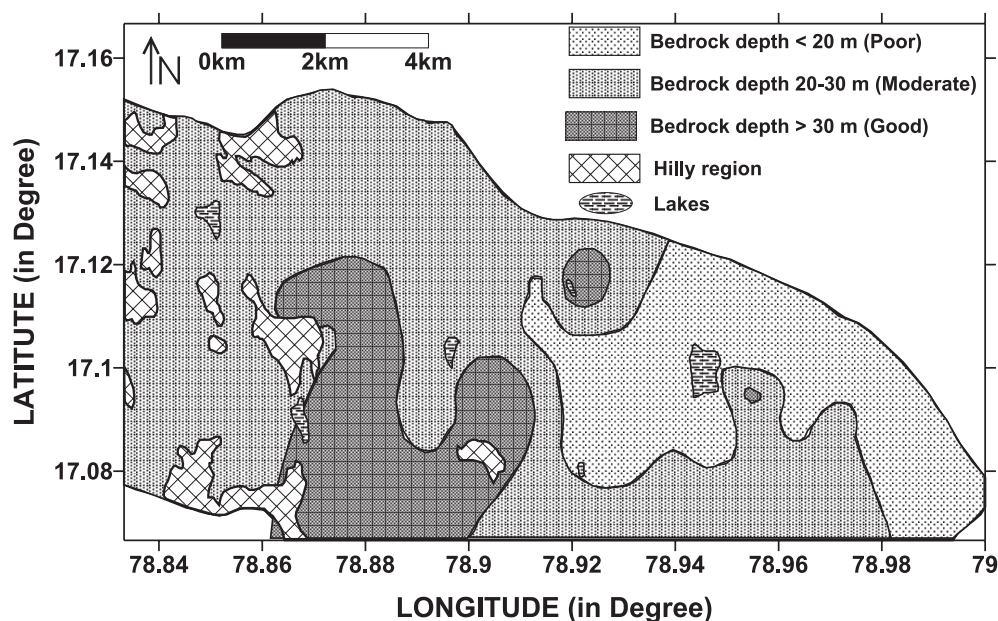


Figure 5: Groundwater potential zone map of the area.



- on sub-surface geoelectric parameters. *Journal of Hydrology*, **299**: 67-83.
- Jupp, D.L.B. and K. Vozoff (1975). Stable iterative methods of inversion of geophysical data. *Geophy. J. Ras.*, **4** (Implemented by T. Harinarayana on VAX 11/750 at NGRI).
- Keller, G.V. and F.C. Frishcknecht (1966). Electrical methods in Geophysical prospecting. Pergamon, London, p. 517.
- Maillet, R. (1947). The fundamental equations of electrical prospecting. *Geophysics*, **12**: 529-556.
- Orellana, E. and H.M. Mooney (1966). Master tables and curves for vertical electrical sounding over layered structures. Interciencia, Madrid, Spain, p. 150 (66 tables).
- Todd, D.K. (1959). Groundwater hydrology. Wiley, New York, p. 538.
- Yadav, G.S. and T. Lal (1989). Investigation of groundwater resources at selected levels in drought prone area of Pahari block, Mirzapur District, U.P., India. *In*: International Workshop Appropriate Methodology, Development, Management Groundwater Resources in Developing Countries, Vol. 1. NGRI, Hyderabad, India, 28 February-4 March 1989, pp. 209-219.
- Zohdy, A.A.R. (1974). Application of surface geophysics to groundwater investigations. US Dept Interior, Geological Survey Book No. 2.

## Contents

Reduction in Methane Emission from Kerala Estuaries	<i>E.J. Zachariah and C.J. Johny</i>	1
Identification of Contamination Sources of an Urban Grown Vegetable Using Factor and Cluster Analyses	<i>F.S. Olise, O.K. Owoade and H.B. Olaniyi</i>	7
Minimization of Freshwater Extraction by Using Treated Wastewater: A Fuzzy-Based Approach	<i>Shakhawat Chowdhury and Tahir Husain</i>	13
A Household Based Safe Water Intervention Programme for a Slum Area in Bangladesh	<i>S.K. Saha, Safina Naznin and Firoj Ahmed</i>	21
Impact of Air Pollution on Health in Klang Valley, Malaysia	<i>Rafia Afroz, Mohd Nasir Hassan, Muhamad Awang and Noor Akma Ibrahim</i>	27
Municipal Waste Management and Environmental Hazards in Bangladesh	<i>G.M. Jahid Hasan and Md. Aktarul Islam Chowdhury</i>	39
Changing Trends of Water Level and Runoff during Past 100 Years of the Yangtze River (China)	<i>Qiang Zhang, Tong Jiang and Chunling Liu</i>	49
Bioremediation of Contaminated Lake Sediments and Evaluation of Maturity Indices as Indicators of Compost Stability	<i>Rekha P., D.S. Suman Raj, C. Aparna, V. Hima Bindu and Y. Anjaneyulu</i>	57
Leachate Quality of Municipal Solid Waste Dumpsites at Chennai, India	<i>S. Esakku, A. Selvam, K. Palanivelu, R. Nagendran and Kurian Joseph</i>	69
An Alternative for Sustainable Domestic Wastewater Treatment in Bangkok	<i>Rabindra Raj Giri, Hiroaki Ozaki and Junichi Takeuchi</i>	77
Environmental Assessment of Tannery Wastes from Chittagong, Bangladesh	<i>Pranab Das, Biplob Das and Yusuf Sharif Ahmed Khan</i>	83
Rhizofiltration of Heavy Metals from Coal Ash Leachate	<i>Madhura Karkhanis, Chotu Jadia and M.H. Fulekar</i>	91
Distribution of Planktonic Foraminifera in the Recent Subtropical Water Mass and their Comparison to the Surface Sediment: Implications for Palaeoenvironmental Reconstruction	<i>Mia Mohammad Mohiuddin</i>	95
Evaluation of Domestic Wastewater Treatment Using Various Natural Filter Media	<i>R. Arthur James, K.V. Emmanuel, Rose Scaria and K. Thanasekaran</i>	103
Autoregressive Model for Flood Forecasting	<i>Sutapa Chaudhuri and Surajit Chattopadhyay</i>	111
□ <i>Research Notes</i>		
Box–Behnken Design of Experiments in the Adsorption of Anionic Dyes on the Bio Polymer Chitosan	<i>N. Sivakumar, R. Basker and R. Sridhar</i>	115
Air Pollution Control in Iran with Special References to Iranian Oil Industry	<i>A.R. Dahaghin, H. Kazemi and S.Tasharrofi</i>	121
Evaluation of Zinc Use Efficiency Using <sup>65</sup> Zn Radiotracer Technique in an Alfisol of Turmeric Crop ( <i>Curcuma longa</i> Var.)	<i>Senthil Kumar Selvaradjou, S. Aruna Geetha, A. Rajarajan, P. Savithri and S. Anthoni Raj</i>	127
Arsenic Removal from Water: A Review	<i>Meenakshi and R.C. Maheshwari</i>	133
The Effect of Climate on the Growth of Paddy	<i>Trilochan Swain</i>	141
Role of Electrical Conductivity as an Indicator of Pollution in Shallow Lakes	<i>Rajib Das, Nihar Ranjan Samal, Pankaj Kumar Roy and Debojyoti Mitra</i>	143
□ <i>Scientific Review</i>		
An Appraisal of Globalization and Sustainable Development for European Countries	<i>Manouchehr Vaziri and Amir Abbas Rassafi</i>	147